Electronic Supplementary Material (ESI) for Physical Chemistry Chemical Physics


# Supporting Information

# Switching from Ru to Fe: picosecond IR spectroscopic interrogation of the potential of the (fulvalene)tetracarbonyldiiron frame for molecular solar-thermal storage

**Zongrui Hou, Son C. Nguyen, Justin P. Lomont, Charles B. Harris, Nikolai Vinokurov and K. Peter C. Vollhardt***

*Department of Chemistry, University of California at Berkeley, Berkeley, CA 94720-1460, USA. E-mail: kpcv@berkeley.edu; Fax: 510.643.5208; Tel: 510.642.0286*

## General

All manipulations were performed using standard Schlenk techniques (Ar) or in a nitrogen atmosphere glove box. Tetrahydrofuran (THF), dimethoxyethane (DME), diethyl ether ($Et_2O$), and *o*-xylene were distilled from sodium/benzophenone prior to use, hexane from $CaCl_2$. $^1H$ and $^{13}C$ NMR spectra were collected on a Bruker AV-600 spectrometer, $^{31}P$ NMR data on an AVQ-400 instrument. All chemical shifts are referenced relative to the residual proton resonance of the deuterated solvent in ppm. All coupling constants are reported in Hertz (Hz). Mass analyses were acquired at the UC Berkeley Mass Spectrometry Laboratory. IR spectra were recorded on a Perkin Elmer Spectrum 100 FT-IR Spectrometer. UV/VIS spectra were obtained on a Perkin Elmer Lambda 35 UV/VIS Spectrometer. Melting points were measured using a capillary melting point apparatus and were not corrected.

## 1. Syntheses of Complexes

### $(\eta^5:\eta^5\text{-}C_{10}H_8)Fe_2(CO)_4$ (3a)

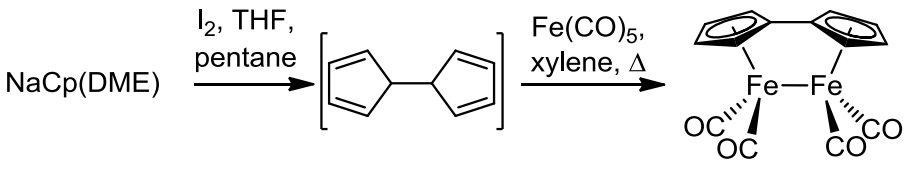


**3a**

To an Ar protected Schlenk flask was added NaCp(DME) (1.78 g, 10 mmol) and THF (30 mL). After cooling to –78 $^oC$, $I_2$ (1.14 g, 4.49 mmol) in THF (10 mL) was injected. The cooling bath

was removed and the reaction mixture allowed to warm to r.t. over exactly 25 min. Degassed pentane (40 mL) and aqueous $Na_2S_2O_3$ (1%, 40 mL) were added and the solutions transferred to an Ar protected separatory funnel. After extraction, the organic layer was transferred to an Ar protected Schlenk flask and cooled to –78 $^oC$. The entire work-up procedure should be performed in less than 5 min, to minimize the decomposition of dihydrofulvalene. This solution was then transferred by cannula under Ar over 1 h into a solution of $Fe(CO)_5$ (6 mL, 90 mmol) in degassed, boiling *o*-xylene (60 mL) that had been heated for 1 min. During this addition, the condenser was cooled by circulating air (not water) to allow the relatively volatile pentane and THF to evaporate and be collected in a receiving flask. After completion of this operation, heating was continued for 10 min, after which the cooling medium of the condenser changed to water and boiling sustained for an additional 20 h. A schematic of the set up is shown below.

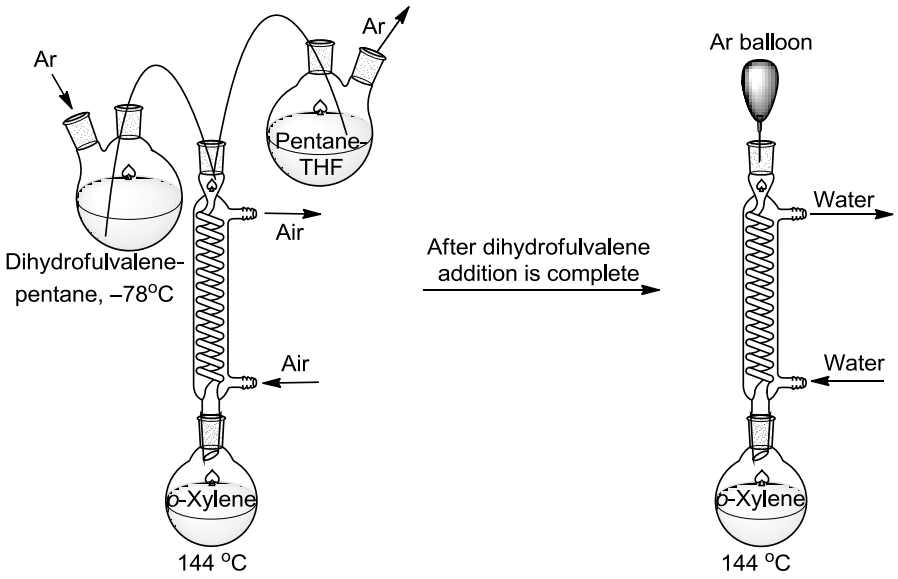


After cooling to r.t., the reaction mixture was filtered through alumina, the solvent removed, and the residue chromatographed on alumina, eluting with $Et_2O$ and hexane (gradient 1:2 to 1:1), all operations under Ar, to afford **3a** (600 mg, 34.1%) as a red solid. Crystallization from $Et_2O$–petroleum ether gave small red crystals suitable for X-ray analysis: NMR spectral data identical to those in the lit.[S1]; IR (crystal) $\tilde{\nu}$ = 2963, 1998, 1927, 1906, 1767, 1430, 1389, 1366, 1035, 1009, 869, 834, 819, 659 $cm^{-1}$; UV/VIS (THF) $\lambda_{max}$ ($\varepsilon$) = 310 (7000), 369 (8150), 450sh (160), endabsorption >600 nm (see also Fig. S1).

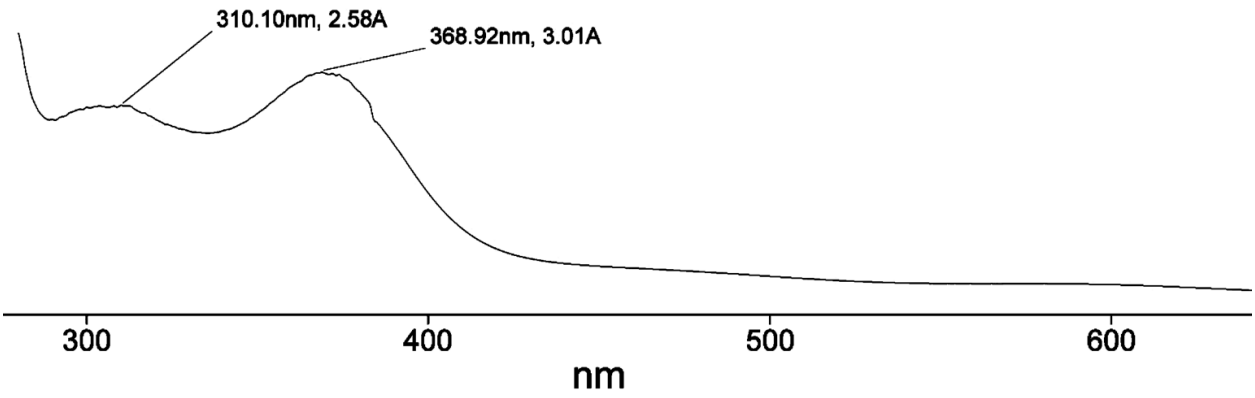


**Fig.** S1 UV spectrum of **3a** in THF.

**($\eta^5$:$\eta^5$-2,2′-*tert*-$Bu_2C_{10}H_6$)$(CO)_4Fe_2$ (3c) and ($\eta^5$:$\eta^5$-2,3′-*tert*-$Bu_2C_{10}H_6$)$(CO)_4Fe_2$ (3d)**

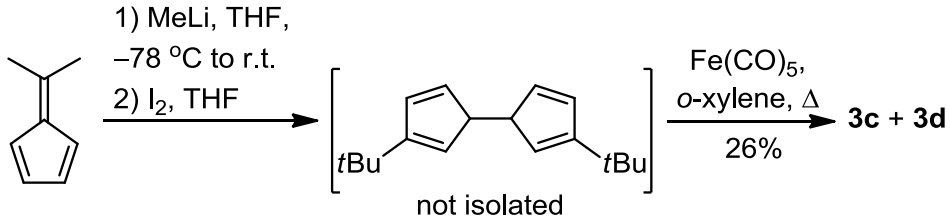


To a solution of 6,6'-dimethylfulvene (0.60 mL, 530.8 mg, 5 mmol) in THF (10 mL) was added MeLi (1.6 M, 3.16 mL, 5.05 mmol) at –78 °C. The mixture was allowed to warm to r.t and stirred for 16 h, during which a white precipitate formed. After renewed cooling to –78 °C, $I_2$ (0.57 g, 2.25 mmol) in THF (6 mL) was injected. The cooling bath was removed, the mixture allowed to warm toward r.t. for exactly 25 min, and degassed pentane (25 mL) was added, followed by degassed aqeuous $Na_2S_2O_3$ (1%, 25 mL). After rapid extraction, the organic layer was washed with degassed brine (25 mL), transferred to an Ar protected Schlenk flask, and cooled rapidly to –78 °C. This solution was then added to boiling *o*-xylene (40 mL) containing $Fe(CO)_5$ (3 mL, 45 mmol) in the same manner as that described for the preparation of **3a**, followed by identical work-up to give **3c**,**d** (1:1) (300 mg, 26%) as a red solid. This mixture was inseparable by chromatography, but was partly enriched in one isomer (**A**:**B** = 3:2 ratio) by crystallization from $Et_2O$-petroleum ether (1:1) under Ar: m.p. 160–170 °C (dec.); $^1$H NMR (600 MHz, THF-$d_8$; the two isomers are designated **A** and **B**): $\delta$ = 5.18 (dd, $J$ = 2.4, 2.4 Hz, 2 H), 4.11

(dd, $J$ = 2.4, 2.4 Hz, 2 H), 3.96 (dd, $J$ = 2.4, 2.4 Hz, 2 H), 1.26 (s, 18 H) ppm; $^{1}$H NMR (600 MHz, $C_6D_6$): $\delta$ = 4.47 (dd, $J$ = 2.4, 2.4 Hz, 2 H), 3.43 (**A**, br s, 1.2 H), 3.39 (**B**, br s, 0.8 H), 3.06 (**B**, br s, 0.8 H), 2.94 (**A**, dd, $J$ = 2.4, 2.4 Hz, 1.2 H), 1.03 (s, 11 H), 1.01 (s, 7 H) ppm; $^{13}$C NMR (150 MHz, THF- $d_8$): $\delta$ = 122.36 (**B**), 121.91 (**A**), 86.97 (2 C), 83.56 (**A**), 83.20 (**B**), 74.51 (**B**), 74.16 (**A**), 73.62 (**A**), 73.23 (**B**), 30.60 (2 C), 30.49 (2 C) ppm (see also Fig. S2), the CO carbon signals could not be detected; IR (crystal) $\tilde{\nu}$ = 2963, 2908, 2871, 1987, 1912, 1773, 1487, 1463, 1395, 1366, 1276, 1155, 1059, 929, 858 cm$^{-1}$; UV/VIS (THF) $\lambda_{max}$ ($\varepsilon$) = 270 (16900), 313 (8100), 370 (10800), 450 (sh, 1600), 550 (sh, 800) nm; HRMS (EI): calcd for $C_{22}H_{24}Fe_2O_4$: 464.0373; found: 464.0380.

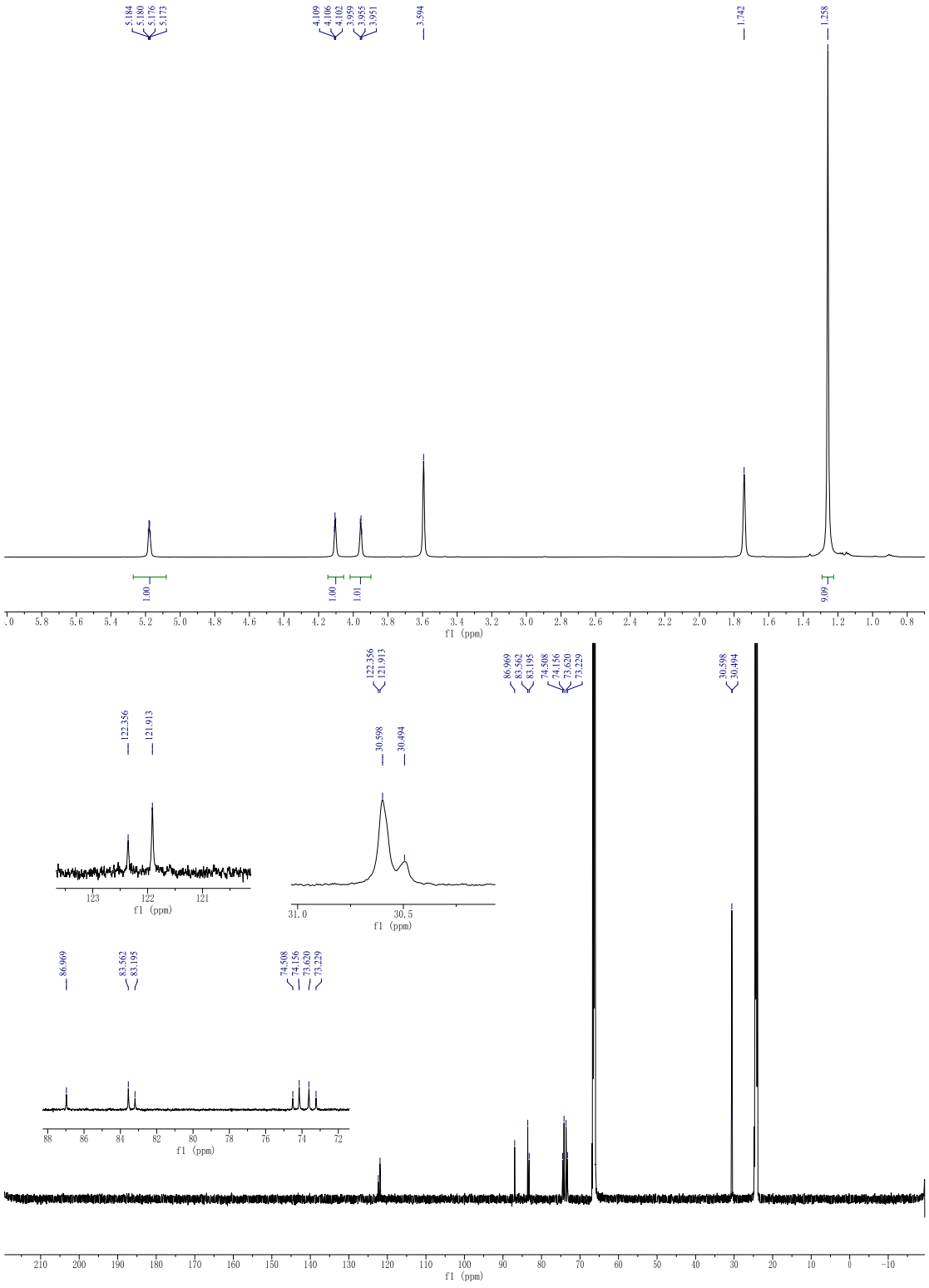
5.184
5.180
5.176
5.173
4.109
4.106
4.102
3.959
3.955
3.951
3.594
1.742
1.258
1.00
1.00
1.01
9.09
f1 (ppm)
122.356
121.913
30.598
30.494
86.969
83.562
83.195
74.508
74.156
73.620
73.229

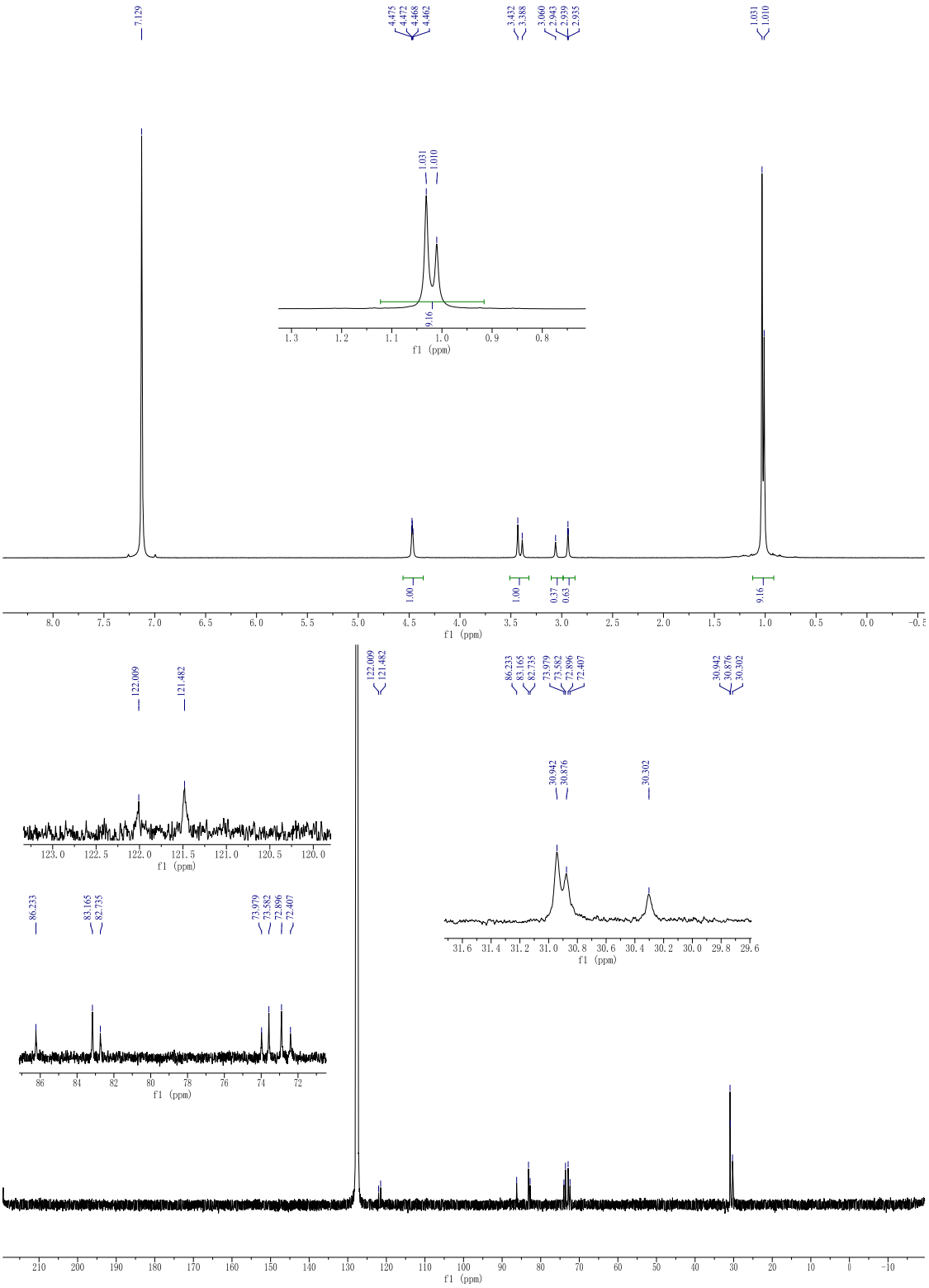

**Fig.** S2 $^{1}H$ and $^{13}C$ NMR spectra of **3c**,**d** in THF-$d_8$ (top) and $C_6D_6$ (bottom), respectively.

## 2. Ultrafast Time-Resolved Infrared Spectroscopy

### Instrumentation and data collection

The ultrafast experimental setup has been described in detail elsewhere.[S2,S3] A commercial Ti:sapphire laser system produces a 1 kHz train of 100 fs, 1.1 mJ pulses centered at 800 nm. This output is split such that 30% is used for the generation of UV/Visible pump pulses [using barium borate (BBO) crystals] at 267 and 400 nm via the third and second harmonic generation of those at 800 nm. The outputs at 267 and 400 nm have powers of 7.2 and 40 $\mu$J per pulse, respectively. They are extended to ~1 ps to avoid multiphoton absorption of the sample and higher order effects in the $CaF_2$ windows. The remainder of the 800 nm output is used to produce the mid-IR pulses in a home-built optical parametric amplifier (OPA), based on the design of Peter Hamm.[S4] About 17% of their power is needed for IR probe and IR reference pulses. The latter are used to eliminate shot-to-shot noise of the laser system. A linear translation stage creates time delays between the UV/Visible excitation and IR probe pulses, the relative polarizations of which are set at the magic angle to avoid the effects of rotational diffusion on the spectra. The pump and probe pulses are then focused and overlapped in a flow sample cell (Harrick), with 2 mm thick $CaF_2$ windows and 930 or 1800 µm polytetrafluoroethene (PTFE) spacers. The cell is moved normal to the IR probe pulses when taking spectra to avoid burning spots on the window. The IR probe and reference pulses are sent to a 150 lines/mm grating spectrograph and then to a 2×32 element MCT array detector with a spectral resolution of ~2.5 $cm^{-1}$. Each spectrum is averaged over $1x10^4$ shots to maximize the signal-to-noise ratio. Samples of **3c**,**d** used to collect TRIR spectra were prepared at a concentration of ~1 mM in heptane in airtight vessels, shielded from ambient light.

### Analysis of TRIR spectra

With 400 nm excitation, the singlet syn biradical photoproduct (species **D**) shows broad bands at 1943, 2008 $cm^{-1}$, decaying with a time constant of 28±2 ps (time constant for the 1943 $cm^{-1}$ band), consistent with the concomitant recovery time of 27±2 ps (time constant for the 1960 $cm^{-1}$ band) of the starting material bleaches at 2015, 1960, 1953 (shoulder) $cm^{-1}$ (Fig. 3). With 267 nm excitation, the analogous time constants are 36±3 (1943 $cm^{-1}$ band) and 39±5 ps (1960 $cm^{-1}$ band), respectively. In the spectra obtained after either 267 or 400 nm excitation, at long delay times (beyond ca. 300 ps), the starting material molecules are not regenerated completely, and

the CO-loss photo product (species **E**) shows constant peak intensities. No other photoproduct is observed in our spectra (up to 1600 ps delay times, Fig. S4).

To calculate the percent of CO-loss product relative to the total number of starting material molecules initially excited, we compare the intensities of the starting material peaks at long delay time (500 ps) to those at 1 ps delay. Due to the spectral overlap of the species **D** with **3c**,**d** at 1ps, Lorentzian fitting is used to obtain accurate intensities for the latter. The fraction of CO-loss product formed is ca. 5% and 10% using 400 and 267 nm excitations, respectively. These values are significantly larger than those for the Ru analog system (< 1% at either 400 or 267 nm excitation).[S2]

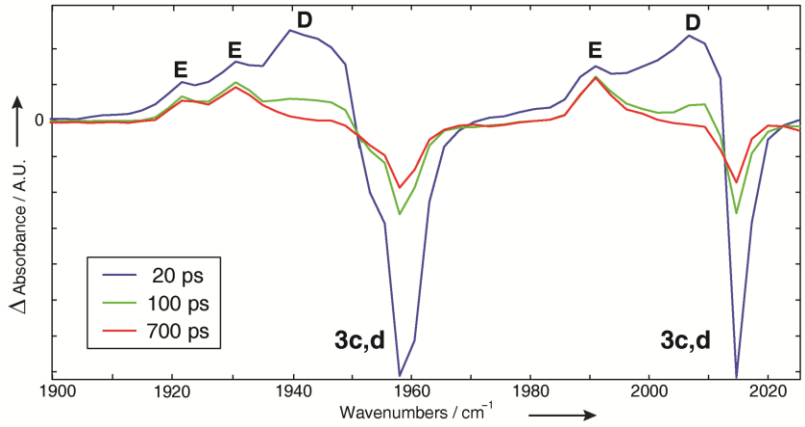


**Fig.** S3 TRIR spectra of **3c**,**d** in heptane after 267 nm excitation.

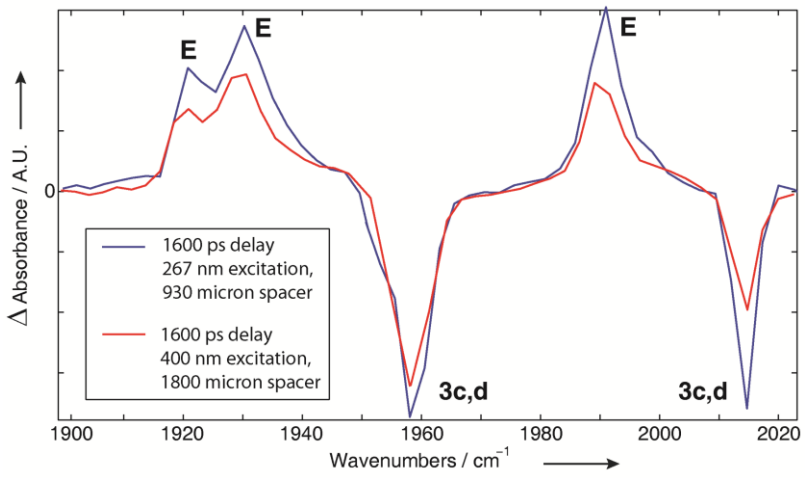


**Fig.** S4 TRIR spectra of **3c**,**d** in heptane after 267 and 400 nm excitations at long delay time. The 400 nm excitation spectra were recorded with a thicker spacer (1800 μm) to improve the signal-to-noise ratio.

## 3. Density Functional Theory Calculations

All calculations are performed with the Gaussian09 software package[S5] using the BP86,[S6] the 6–31+G(d,p) basis set for C, O, and H, and the LANL2DZ[S7] basis set for Fe. This combination has been employed previously and with satisfactory results for other organometallic species.[S2,S8] The structural assignment of the experimentally detected species **E,** *tert*-$Bu_2FvFe_2(CO)_3$, was assisted by DFT calculations of the unsubstituted analog $FvFe_2(CO)_3$ (Fig. S5). This structure was simulated by removing one CO ligand from $FvFe_2(CO)_4$ and subsequent optimization. Figure S6 shows the ground-state structure of triplet $FvFe_2(CO)_4$, the energy of which is reported in Fig. 1.

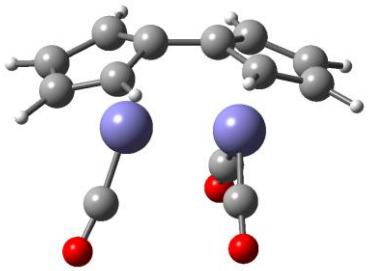

**Fig.** S5 Structure of $FvFe_2(CO)_3$.

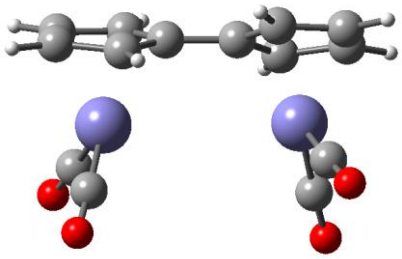

**Fig.** S6 Structure of triplet $FvFe_2(CO)_4$ (**3a**).

### Molecular coordinates

**$FvFe_2(CO)_3$**

| | | | |
|---|---|---|---|
| C | 2.86755300 | -0.73510500 | -0.91687700 |
| C | 0.83359800 | -1.74542000 | -0.33792300 |
| C | 1.59635300 | -1.18006200 | -1.42968700 |
| C | 1.65562100 | -1.62921600 | 0.84609200 |
| C | 2.90186900 | -1.00740900 | 0.48013100 |
| H | 3.65337400 | -0.25298600 | -1.49821400 |
| H | 1.25912400 | -1.08065000 | -2.46114200 |
| H | 1.37273800 | -1.92871700 | 1.85464800 |
| H | 3.71997900 | -0.77272900 | 1.16086800 |

| | | | |
|---|---|---|---|
| C | -2.78432000 | -1.03106700 | -0.69757300 |
| C | -0.62667600 | -1.86353400 | -0.30711600 |
| C | -1.50150100 | -1.25917600 | -1.30979900 |
| C | -1.39990600 | -1.96412400 | 0.90179100 |
| C | -2.71932900 | -1.45345700 | 0.67192900 |
| H | -3.64326600 | -0.57177400 | -1.18733700 |
| H | -1.23730300 | -1.01681800 | -2.33886100 |
| H | -1.01375200 | -2.26971700 | 1.87568800 |
| H | -3.52125200 | -1.39241500 | 1.40711600 |
| Fe | 1.20585600 | 0.28719900 | 0.04036100 |
| Fe | -1.23742300 | 0.03558600 | 0.21570900 |
| C | 1.02794200 | 1.69925700 | -0.95975200 |
| O | 0.95509700 | 2.64255400 | -1.65497300 |
| C | 1.00436400 | 1.22618800 | 1.49407600 |
| O | 0.91752600 | 1.85532100 | 2.48491300 |
| C | -1.93116000 | 1.62164700 | -0.06627600 |
| O | -2.53704200 | 2.60490500 | -0.29052500 |

**Triplet $FvFe_2(CO)_4$**

| | | | |
|---|---|---|---|
| C | 3.04335200 | -1.72101500 | -0.01859700 |
| C | 0.71676800 | -1.53149200 | 0.16071000 |
| C | 1.79563600 | -1.76392800 | -0.76012800 |
| C | 1.30897100 | -1.26638500 | 1.44609500 |
| C | 2.74345800 | -1.42924600 | 1.33902800 |
| H | 4.03614300 | -1.87558300 | -0.44111700 |
| H | 1.69191300 | -2.00427200 | -1.81815700 |
| H | 0.76313900 | -1.02013100 | 2.35739400 |
| H | 3.46186000 | -1.30476900 | 2.14871700 |
| C | -2.74343600 | -1.42927200 | -1.33902900 |
| C | -0.71674700 | -1.53149800 | -0.16071000 |
| C | -1.30895100 | -1.26639900 | -1.44609600 |
| C | -1.79561300 | -1.76393700 | 0.76012900 |
| C | -3.04332800 | -1.72103900 | 0.01859700 |
| H | -3.46183900 | -1.30480100 | -2.14871900 |
| H | -0.76312100 | -1.02014400 | -2.35739600 |
| H | -1.69188900 | -2.00427700 | 1.81815900 |
| H | -4.03611800 | -1.87561200 | 0.44111600 |
| Fe | 2.05330900 | 0.19492500 | 0.05676500 |
| Fe | -2.05330200 | 0.19490900 | -0.05677000 |
| C | 2.96639600 | 1.00586100 | -1.19787800 |
| O | 3.61677600 | 1.52243800 | -2.02639500 |
| C | 2.09447700 | 1.57292400 | 1.13965200 |
| O | 2.15679500 | 2.46968400 | 1.89274400 |
| C | -2.09446400 | 1.57291100 | -1.13965400 |
| O | -2.15686700 | 2.46972200 | -1.89267800 |
| C | -2.96640600 | 1.00583100 | 1.19786900 |

| | | | |
|---|---|---|---|
| O | -3.61682100 | 1.52240900 | 2.02635800 |

## References


S1 H.-J. Bister and H. Butenschön, *Synlett*, 1992, **3**, 22.

S2 M. R. Harpham, S. C. Nguyen, Z. Hou, J. C. Grossman, C. B. Harris, M. W. Mara, A. B. Stickrath, Y. Kanai, A. M. Kolpak, D. Lee, D.-J. Liu, J. P. Lomont, K. Moth-Poulsen, N. Vinokurov, L. X. Chen and K. P. C. Vollhardt, *Angew. Chem.* 2012, **124**, 7812; *Angew. Chem. Int. Ed.*, 2012, **51**, 7692.

S3 J. P. Lomont, S. C. Nguyen and C. B. Harris, *Organometallics*, 2012, **31**, 3947.

S4 P. Hamm, R.A. Kaindl and J. Stenger, *Opt. Lett.*, 2000, **25**, 1798.

S5 Gaussian 09, Revision B.01, M. J. Frisch, G. W. Trucks, H. B. Schlegel, G. E. Scuseria, M. A. Robb, J. R. Cheeseman, G. Scalmani, V. Barone, B. Mennucci, G. A. Petersson, H. Nakatsuji, M. Caricato, X. Li, H. P. Hratchian, A. F. Izmaylov, J. Bloino, G. Zheng, J. L. Sonnenberg, M. Hada, M. Ehara, K. Toyota, R. Fukuda, J. Hasegawa, M. Ishida, T. Nakajima, Y. Honda, O. Kitao, H. Nakai, T. Vreven, J. A. Montgomery, Jr., J. E. Peralta, F. Ogliaro, M. Bearpark, J. J. Heyd, E. Brothers, K. N. Kudin, V. N. Staroverov, T. Keith, R. Kobayashi, J. Normand, K. Raghavachari, A. Rendell, J. C. Burant, S. S. Iyengar, J. Tomasi, M. Cossi, N. Rega, J. M. Millam, M. Klene, J. E. Knox, J. B. Cross, V. Bakken, C. Adamo, J. Jaramillo, R. Gomperts, R. E. Stratmann, O. Yazyev, A. J. Austin, R. Cammi, C. Pomelli, J. W. Ochterski, R. L. Martin, K. Morokuma, V. G. Zakrzewski, G. A. Voth, P. Salvador, J. J. Dannenberg, S. Dapprich, A. D. Daniels, O. Farkas, J. B. Foresman, J. V. Ortiz, J. Cioslowski and D. J. Fox, Gaussian, Inc., Wallingford CT, 2010.

S6 A. D. Becke, *Phys. Rev. A*, 1988, **38**, 3098.

S7 a) P. J. Hay and W. R. Wadt, *J. Chem. Phys.*, 1985, **82**, 299; b) T. H. Dunning and P. J. Hay, in *Methods of Electronic Structure Theory*, *Vol. 2*, ed. H. F. Schaefer, Plenum, New York, 1977.

S8 a) K. R. Sawyer, J. F. Cahoon, J. E. Shanoski, E. A. Glascoe, M. F. Kling, J. P. Schlegel, M. C. Zoerb, M. Hapke, J. F. Hartwig, C. E. Webster and C. B. Harris, *J. Am. Chem. Soc.* 2010, **132**, 1848; b) J. F. Cahoon, K. R. Sawyer, J. P. Schlegel and C. B. Harris, *Science* 2008, **319**, 1820.